

DualFed: Enjoying both Generalization and Personalization in Federated Learning via Hierarchical Representations

Guogang Zhu

buaa_zgg@buaa.edu.cn
State Key Laboratory of Virtual Reality Technology and Systems, School of Computer Science and Engineering, Beihang University Beijing, China

Xuefeng Liu

liu_xuefeng@buaa.edu.cn
State Key Laboratory of Virtual Reality Technology and Systems, School of Computer Science and Engineering, Beihang University Beijing, China
Zhongguancun Laboratory Beijing, China

Jianwei Niu*

niu Jianwei@buaa.edu.cn
State Key Laboratory of Virtual Reality Technology and Systems, School of Computer Science and Engineering, Beihang University Beijing, China
Zhongguancun Laboratory Beijing, China

Shaojie Tang

shaojiet@buffalo.edu
Department of Management Science and Systems, University at Buffalo Buffalo, New York, United States

Xinghao Wu

wuxinghao@buaa.edu.cn
State Key Laboratory of Virtual Reality Technology and Systems, School of Computer Science and Engineering, Beihang University Beijing, China

Jiayuan Zhang

zhangjiayuan@buaa.edu.cn
State Key Laboratory of Virtual Reality Technology and Systems, School of Computer Science and Engineering, Beihang University Beijing, China

Abstract

In personalized federated learning (PFL), it is widely recognized that achieving both high model generalization and effective personalization poses a significant challenge due to their conflicting nature. As a result, existing PFL methods can only manage a trade-off between these two objectives. This raises an interesting question: *Is it feasible to develop a model capable of achieving both objectives simultaneously?* Our paper presents an affirmative answer, and the key lies in the observation that deep models inherently exhibit hierarchical architectures, which produce representations with various levels of generalization and personalization at different stages. A straightforward approach stemming from this observation is to select multiple representations from these layers and combine them to concurrently achieve generalization and personalization. However, the number of candidate representations is commonly huge, which makes this method infeasible due to high computational costs. To address this problem, we propose DualFed, a new method that can directly yield dual representations correspond to generalization and personalization respectively, thereby simplifying the optimization task. Specifically, DualFed inserts a personalized projection network between the encoder and classifier. The pre-projection representations are able to capture generalized information shareable across clients, and the post-projection representations are effective

to capture task-specific information on local clients. This design minimizes the mutual interference between generalization and personalization, thereby achieving a win-win situation. Extensive experiments show that DualFed can outperform other FL methods. Code is available at <https://github.com/GuogangZhu/DualFed>.

CCS Concepts

• **Computing methodologies** → **Distributed artificial intelligence**.

Keywords

Federated Learning, Generalization, Personalization, Representation Learning

ACM Reference Format:

Guogang Zhu, Xuefeng Liu, Jianwei Niu, Shaojie Tang, Xinghao Wu, and Jiayuan Zhang. 2024. DualFed: Enjoying both Generalization and Personalization in Federated Learning via Hierarchical Representations. In *Proceedings of the 32nd ACM International Conference on Multimedia (MM '24)*, October 28–November 1, 2024, Melbourne, VIC, Australia. ACM, New York, NY, USA, 15 pages. <https://doi.org/10.1145/3664647.3681260>

1 Introduction

Federated learning (FL) [37] is an emerging machine learning paradigm that enables multiple clients to collaboratively train a model while preserving their data privacy. In real-world applications, data distributions across clients are often non-independent and identically distributed (Non-IID). For instance, in video surveillance, the data collected by distributed cameras can vary significantly due to differences in weather and lighting conditions [7, 17, 25, 38]. This Non-IID data distributions can significantly degrade the FL model performance [66, 72]. Currently, there are primarily two objectives to mitigate this issue: improving model generalization to accommodate more clients or enhancing model personalization

*Corresponding Author.

Permission to make digital or hard copies of all or part of this work for personal or classroom use is granted without fee provided that copies are not made or distributed for profit or commercial advantage and that copies bear this notice and the full citation on the first page. Copyrights for components of this work owned by others than the author(s) must be honored. Abstracting with credit is permitted. To copy otherwise, or republish, to post on servers or to redistribute to lists, requires prior specific permission and/or a fee. Request permissions from permissions@acm.org.
MM '24, October 28–November 1, 2024, Melbourne, VIC, Australia

© 2024 Copyright held by the owner/author(s). Publication rights licensed to ACM.
ACM ISBN 979-8-4007-0686-8/24/10
<https://doi.org/10.1145/3664647.3681260>

to better adapt local data distributions. However, since local data distributions often differ from the global distribution in Non-IID FL, these two optimized objectives are typically in conflict.

Personalized federated learning (PFL), which aims to balance model generalization with personalization, serves as an effective approach to address the challenges posed by Non-IID data. Earlier PFL approaches suggest sharing the classifier or encoder, while personalizing the other [1, 11, 32]. This strategy aims to strike a balance between client collaboration and local adaptation, as presented in Figure 1 (a) and (b). However, these approaches can only ensure that the encoder to generate either the generalized or personalized representations. Thereby, some PFL methods suggest personalizing specific parameters within the encoder, allowing it to extract the representations that exhibit both generalization and personalization [29, 47, 49]. Additionally, some PFL techniques concurrently use global and personalized classifiers for predictions [6, 65] to harmonize generalization and personalization. Nevertheless, these methods inherently involve a trade-off between model generalization and personalization. This leads to an interesting question: *Is it feasible to create a model that can achieve both of these objectives concurrently in Non-IID FL?*

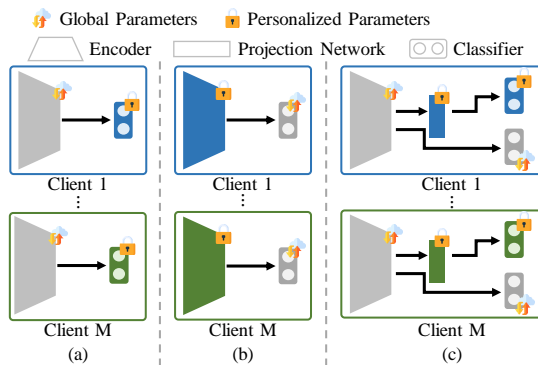


Figure 1: Different forms that combines the representations and the classifier. (a) Global encoder with personalized classifier, (b) Personalized classifier with global encoder, (c) Our proposed DualFed that utilizes hierarchical representations.

In fact, the dilemma in existed PFL methods primarily because they rely solely on post-encoder representations for decision-making. This design presents a significant hurdle as it necessitates the post-encoder representations to simultaneously exhibit both high generalization and personalization – objectives that are inherently contradictory in Non-IID FL. It is well known that deep models naturally produce hierarchical representations, as evidenced in studies such as [2, 16, 36, 40, 44, 48, 54, 61, 63]. The shallow layers capture general patterns that are transferable across different data distributions. As we delve into deeper layers, the representations become more specified for the downstream task. This implies that both the generalization and personalization that PFL seeks for are already existed within the model. These observations do shed some lights on us: *Can we leverage the hierarchical representations within the deep model to achieve both high model generalization and personalization simultaneously?*

In this paper, we provide a positive response to the question posed earlier. A straightforward method for leveraging hierarchical representations involves directly selecting both generalized and personalized representations from them. However, this approach can incur substantial computational costs, owing to the volume of the candidate representations [45]. To address this problem, we introduce DualFed, a new PFL approach that not only straightforward to implement but also effectively decouple these two types of representations. As shown in Figure 1 (c), in DualFed, we modify the commonly used encoder-classifier architecture by inserting a projection network between the encoder and classifier. This modification generates representations at two distinct stages, aligning with the objectives of generalization and personalization, respectively. Specifically, the *pre-projection representations* generated before the projection network, are isolated from local tasks, making them more transferable across clients. Conversely, the *post-projection representations* produced after the projection network are closer to the decision layers, being more discriminative and personalized to local data distributions. To align with the objectives of these two representations, we maintain a shared encoder while localizing the projection network. A global classifier and a personalized classifier are trained using the pre-projection and post-projection representations, respectively. During inference, the outputs from these two classifier are combined to yield the final predictions, effectively benefiting from collaboration across clients and local adaptation.

We conduct extensive experiments on multiple datasets to demonstrate the effectiveness of DualFed. The experimental results show that DualFed can outperform state-of-the-art (SOTA) FL methods.

2 Related Work

Federated Learning. FL [20, 27] can be categorized into general FL (GFL) [21, 28, 37] and personalized FL (PFL) [1, 11, 29, 32, 49, 50, 56–58, 67]. GFL aims to develop a generalized model that can be shared across clients. However, in Non-IID FL, it becomes challenging for a global model to satisfy the diverse needs of multiple clients, often leading to significant performance degradation [66, 72]. Consequently, PFL has emerged as an effective solution for these Non-IID situations by introducing model personalization to better align with local data distributions. There are various approaches to implement PFL, including model clustering [3, 4, 14, 46], and the personalization of specific parameters within the model [1, 11, 29, 32, 49]. However, these PFL methods can only manage a trade-off between model generalization and personalization, as they expect the post-encoder representations to achieve the conflicting objectives.

Representation Learning in Deep Models. Since advanced deep learning models are typically organized as hierarchical layers, analysing how representations evolve during the representation extraction process has been an established field [36, 40, 54, 61, 63]. Previous research indicates that deep models start by extracting generalized features and progressively filter out irrelevant components, retaining only those crucial for downstream tasks [36, 61]. This has inspired numerous studies that leverage intermediate representations, in domains like object detection [33]. However, selecting the optimal representations for each specific problem is computationally challenging [45]. In response, SimCLR [8] proposes to use a scalable projection network during training and

discard it afterwards. This design has become a common practice in both supervised learning [13, 22, 55] and self-supervised learning [5, 9, 10, 15, 62]. Since then, numerous studies have explored the projector’s role in model training from empirical [2, 30, 45, 55] and theoretical perspectives [19, 54, 59]. The common explanation is that the projection network differentiates the representations of the pre-training and downstream tasks, thereby enhancing the model transferability [55]. This situation is especially significant when the pre-training and downstream tasks are misaligned [2]. Nevertheless, the effects of projection network within FL are still not fully understood.

Federated Learning within Representation Space. The primary contribution of these methods is the regularization of the representation space to mitigate data heterogeneity [34, 35, 43, 51, 64, 65, 68, 69]. A straightforward strategy in these approaches involves directly calibrating the representation space. For instance, CCVR [35] post-calibrates the classifier after federated training using virtual representations. Another research direction links performance degradation to the misalignment of representation spaces across clients [68, 69]. In response, various methods have been developed to explicitly align the representation space across clients. Notably, FedProto [51], AlignFed [69, 70], and FedFA [68] use class-wise representation centers for representation alignment. Additionally, some methods achieve alignment by implementing a fixed classifier. For instance, FedBABU [39] employs a randomly initialized classifier, SphereFed [12] introduces an orthogonal classifier, while FedETF [31] implements an ETF (Equiangular Tight Frame) classifier during model training. However, these methods primarily focus on extracting generalized representations shareable across clients, often overlooking the personalized representations specific to local tasks. Consequently, recent studies have focused on balancing both model generalization and personalization [6, 71]. For example, Fed-RoD [6] achieving this goal combining the predictions of personalized and global classifiers. Yet, these methods face challenges, as they rely solely on representations at the same stage. Expecting the single-stage representations to exhibit both generalization and personalization is often intertwined.

3 Preliminaries

3.1 Federated Learning

In this paper, we consider a standard PFL setting which consists of a central server and M distributed clients. For each client $m \in [M]$, there are totally N_m samples $\{\mathbf{x}_m^i, \mathbf{y}_m^i\}_{i=1}^{N_m}$ drawn from the distribution \mathcal{D}_m , where $\mathbf{x}_m^i \in \mathcal{X}_m \subseteq \mathbb{R}^n$ represents the raw input and $\mathbf{y}_m^i \in \mathcal{Y}_m \subseteq \{0, 1\}^C$ represents the corresponding label, with C denoting the total number of classes. In Non-IID scenarios within PFL, the data distributions are assumed to be heterogeneous across clients, indicating that $\mathcal{D}_i \neq \mathcal{D}_j, \forall i, j \in \{1, 2, \dots, M\}, i \neq j$.

The goal of a standard PFL setting is to develop a model $\psi_m(\cdot)$ parameterized by Θ_m for client m . The corresponding optimization objective can be expressed as:

$$\arg \min_{\Theta_1, \dots, \Theta_M} \mathcal{L}(\Theta_1, \dots, \Theta_M) \triangleq \arg \min_{\Theta_1, \dots, \Theta_M} \frac{1}{M} \sum_{m=1}^M \mathcal{L}_m(\Theta_m), \quad (1)$$

where $\mathcal{L}(\Theta_1, \dots, \Theta_M)$ represents the overall optimization objective for the PFL system, $\mathcal{L}_m(\Theta_m)$ denotes the empirical risk for client m .

In PFL, directly optimizing $\mathcal{L}(\Theta_1, \dots, \Theta_M)$ is commonly infeasible as the clients cannot access the data on other clients. Therefore, a PFL training procedure typically involves the independently local updating performed on participating clients utilizing their own empirical risk and the model aggregation performed on the server. Specifically, for client m , its empirical risk is defined as:

$$\mathcal{L}_m(\Theta_m) := \frac{1}{N_m} \sum_{i=1}^{N_m} \ell(\mathbf{y}_m^i, \hat{\mathbf{y}}_m^i), \quad (2)$$

with $\hat{\mathbf{y}}_m^i = \psi_m(\mathbf{x}_m^i; \Theta_m)$ representing the model’s prediction for \mathbf{x}_m^i , and $\ell: \mathcal{Y} \times \mathcal{Y} \rightarrow \mathbb{R}$ being the loss function that quantifies the prediction error (e.g., cross-entropy loss).

Once the local training on clients is completed, the participating clients upload their updated global parameters within the model to the server. The server then averages the parameters at corresponding positions to generate new global parameters. These global parameters are subsequently distributed to the clients for the next round of local updating. By iteratively performing local training and model aggregation, PFL facilitates collaborative model training without the need to share raw data from the clients.

For the sake of brevity, we occasionally omit the superscript denoting the sample index in subsequent sections of this paper. Additionally, we sometimes denote personalized parameters with the superscript p (e.g., Θ_m^p), and global parameters with the superscript s (e.g., Θ_m^s), to clarify the expressions in the following sections.

3.2 Motivation of DualFed

As shown Figure 1 (a) and (b), in previous studies of PFL, the model Θ_m is commonly divided into an encoder $f_m(\cdot)$ and a classifier $h_m(\cdot)$ [1, 11, 39, 68, 69], parameterized by θ_m^f and θ_m^h , respectively. The encoder $f_m(\cdot): \mathcal{X}_m \rightarrow \mathcal{Z}_m$ generally consists of a series of stacked convolutional layers. It maps the raw input \mathbf{x}_m from $\mathcal{X}_m \subseteq \mathbb{R}^n$ into a representation space $\mathcal{Z}_m \subseteq \mathbb{R}^k$, which is denoted as $\mathbf{z}_m = f(\mathbf{x}_m; \theta_m^f)$. Here, $\mathbf{z}_m \in \mathcal{Z}_m$ denotes the representation generated from \mathbf{x}_m utilizing the encoder $f_m(\cdot)$. Practically, the dimension of this representation is significantly smaller than that of the raw input, which implies that $k \ll n$. The classifier, $h_m(\cdot): \mathcal{Z}_m \rightarrow \mathcal{Y}_m$, generally includes a fully connected (FC) layer and a softmax layer. It generates the normalized predictions $\hat{\mathbf{y}}_m$ based on the representation \mathbf{z}_m , which is indicated as $\hat{\mathbf{y}}_m = h_m(\mathbf{z}_m; \theta_m^h)$.

Nevertheless, within the encoder-classifier architecture, only the representations after the encoder, referred to as the **post-encoder representations**, are used for decision-making. This approach can lead to a dilemma in PFL, as generalization and personalization are contradictory objectives, particularly in Non-IID scenarios. More specifically, to enhance model generalization, the post-encoder representations should capture shared information across varying data distributions among clients. On the other hand, enhancing model personalization requires these representations to capture specific information aligned with each client’s local data distribution. When the data distribution varies significantly across clients, these two types of information can be vastly different. Consequently, in this encoder-classifier architecture, ensuring that the post-encoder representations simultaneously meet these two conflicting objectives is a challenging task.

To address the dilemma mentioned earlier, we shift our focus on the process of representation extraction within the deep models. Advanced deep models are typically organized in a hierarchical architecture. As shown in previous studies, these models initially extract generalized representations that are transferable across various data distributions [2, 16, 36, 40, 44, 48, 54, 61, 63]. As the model progresses to deeper layers, it gradually discards irrelevant components and retains only information relevant to the specific task. In other words, both the generalized and personalized representations that PFL seeks for are already existed within the model. By leveraging these hidden generalized and personalized representations, we can achieve both high generalization and personalization in PFL. However, directly extracting these specific representations during the representation extraction phase is computationally challenging [45]. Therefore, DualFed adopts a simpler strategy by incorporating a personalized projection network, which effectively decouples the generalized and personalized representations.

4 Method

4.1 Framework Overview of DualFed

Figure 2 presents the framework of DualFed. It aligns with the standard training framework of PFL, which includes iterative local training on clients and global model aggregation on the server. The key innovation in DualFed, as compared to previous PFL methods, is the integration of a personalized projection network situated between the encoder and the classifier. We refer to this personalized projection network as $g_m^p(\cdot)$, with its parameters denoted by $\theta_m^{g,p}$. Functionally, this projection network, $g_m^p(\cdot) : \mathcal{Z}_m \rightarrow \mathcal{U}_m$ is usually a MLP (multi-layer perceptron). By inserting this projection network, the representations produced by the encoder are not directly inputted into the classifier for prediction. Instead, they first pass through the projection network, which remaps them to a personalized representation space $\mathcal{U}_m \subseteq \mathbb{R}^d$. Formally, we represent this process as $\mathbf{u}_m = g(\mathbf{z}_m; \theta_m^{g,p})$. For clarity, we term the representation before the projection network (i.e., \mathbf{z}_m) as the **pre-projection representations**, and the representation after the projection network (i.e., \mathbf{u}_m) as the **post-projection representations**.

Drawing on the hierarchical nature of deep model representation extraction, the pre-projection and post-projection representations in our framework exhibit distinct characteristics, aligning with the generalized and personalized objectives of PFL, respectively. Specifically, the pre-projection representations are separated from the final outputs by the projector network, meaning that they are not directly tied to the local tasks on each client. As previously studies have shown, these pre-projection representations are easier transferred across different data distributions [45, 55]. Therefore, in DualFed, the post-projection representations are fed into a global classifier $h_m^s(\cdot)$, which is parameterized by $\theta_m^{h,s}$. Additionally, to encourage the encoder to extract more generalized information, we let the encoder be shared among clients in DualFed. The predictions from this global classifier is expressed as:

$$\hat{\mathbf{y}}_m^s = h_m^s \circ f_m^s(\mathbf{x}_m), \forall m \in [M]. \quad (3)$$

Conversely, the post-projection representations are more closely aligned with the final outputs. This implies that these representations are more pertinent to accomplishing tasks related to the local

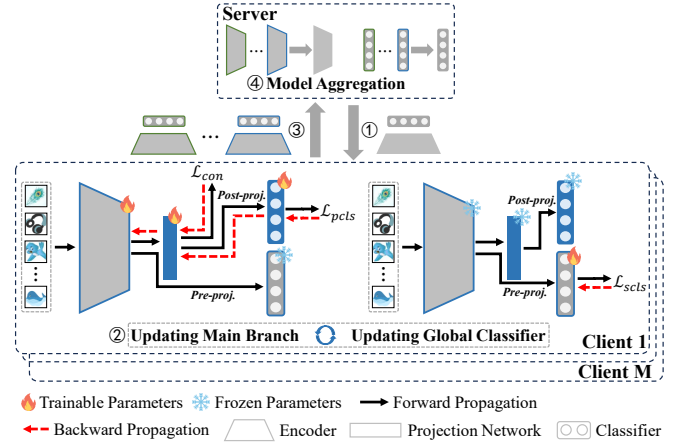


Figure 2: Framework overview of DualFed. It consists of 4 steps in a single global round: 1) the server broadcasts global encoder and classifier to each client; 2) each client performs local updating by iteratively updating main branch and global classifier; 3) each client uploads its updated global encoder and classifier to the server; 4) the server aggregates encoders and classifiers from clients to generate new ones.

data distribution. In DualFed, to effectively adapt to these local distributions, we utilize a personalized classifier $h_m^p(\cdot)$ for each client, parameterized by $\theta_m^{h,p}$, to adapt to the local data distribution. For a given input \mathbf{x}_m , the prediction generated by this personalized classifier can be expressed as follows:

$$\hat{\mathbf{y}}_m^p = h_m^p \circ g_m^p \circ f_m^s(\mathbf{x}_m), \forall m \in [M]. \quad (4)$$

During inference, the final predictions are derived by ensembling the outputs from both the global classifier and the personalized classifier. This process is expressed as follows:

$$\hat{\mathbf{y}}_m = \hat{\mathbf{y}}_m^p + \hat{\mathbf{y}}_m^s, \forall m \in [M]. \quad (5)$$

By integrating a personalized projection network between the encoder and the classifier, DualFed effectively separates the contradictory optimization objectives inherent in PFL into distinct stages within the model. This approach resolves the conflict of pursuing contradictory objectives within the representations in the same stage, thereby can achieve a win-win situation between the model generalization and personalization.

4.2 Local Training on Client

In DualFed, each client updates the model for E rounds using its own datasets after receiving the global models from the sever. In order to fully exploit the hierarchical characteristics of deep model representations and achieve the optimization objectives of PFL, we introduce a stage-wise training procedure for local clients.

At the first stage, we freeze the global classifier and training the main branch of the model. The main branch comprises the global encoder, the personalized projector, and the personalized classifier, with their parameters collectively represented as $\bar{\Theta}_m :=$

$\{\theta_m^{f,s}, \theta_m^{g,p}, \theta_m^{h,p}\}$. This stage allows the model to extract both generalized and personalized representations. To ensure the model's effectiveness in accomplishing local tasks, we employ cross-entropy loss as the classification loss, as indicated in the following equation:

$$\mathcal{L}_{pcls} = \sum_{i=1}^{N_m} \sum_{c=1}^C \mathbf{y}_m^{i,c} \log(\hat{\mathbf{y}}_m^{p,i,c}), \quad (6)$$

where $\mathbf{y}_m^{i,c}$ denotes the value at c^{th} class of the one-hot ground-truth label of the i^{th} sample on client m , $\hat{\mathbf{y}}_m^{p,i,c}$ represents the normalized prediction probability of c^{th} classes of the i^{th} sample on client m from the personalized classifier.

As the post-projection representations are tailored to adapt to the local data distribution, we further enhance its discrimination by implementing supervised contrastive loss [22], as demonstrated in the following equation:

$$\mathcal{L}_{con} = -\frac{1}{N_m} \sum_{i=1}^{N_m} \frac{1}{|A(i)|} \sum_{j \in A(i)} \log \frac{\exp(\mathbf{u}_i \odot \mathbf{u}_j / \tau)}{\sum_{a \in A \setminus \{i\}} \exp(\mathbf{u}_i \odot \mathbf{u}_a / \tau)} \quad (7)$$

where A is the full set of samples, $A(i)$ consists of samples in A that belong to the same class as \mathbf{x}_m^i , \odot is the cosine similarity, and $\tau \in \mathcal{R}^+$ is the temperature coefficient.

The optimization objective at this stage is then defined as:

$$\bar{\Theta}_m^t = \arg \min_{\Theta_m} \mathcal{L}_{pcls} + \lambda \mathcal{L}_{con}. \quad (8)$$

where λ denotes the hyperparameter used for balancing these two loss terms, t denotes the local updating epochs.

After updating $\bar{\Theta}_m$, we freeze its parameters and train the global classifier using the pre-projection representations to fulfill the local task, as represented in the following equation:

$$\mathcal{L}_{scls} = \sum_{i=1}^{N_m} \sum_{c=1}^C \mathbf{y}_m^{i,c} \log(\hat{\mathbf{y}}_m^{s,i,c}), \quad (9)$$

where $\mathbf{y}_m^{i,c}$ denotes the value at c class of the one-hot ground-truth label of the i_{th} sample on client m , $\hat{\mathbf{y}}_m^{s,i,c}$ represents the normalized prediction probability of c classes of the i_{th} sample on client m from the global classifier.

The optimization objective in this stage can be expressed as:

$$\theta_m^{h,s,t} = \arg \min_{\theta_m^{h,s}} \mathcal{L}_{scls}. \quad (10)$$

In DualFed, both optimization objectives, as described in Eqs. (8) and (10), are optimized using mini-batch stochastic gradient descent (SGD). As evidenced by our experiments, this stage-wise optimization strategy diminishes the impact of local tasks on the pre-projection representations, thereby effectively preserving its generalization.

4.3 Model Aggregation on Server

Once the local updating process is complete, the clients send their global encoder and classifier parameters to the server. The server then aggregates these parameters using the following equation:

$$\tilde{\theta}^{f,s} = \sum_{m=1}^M \frac{1}{M} \theta_m^{f,s}, \quad \tilde{\theta}^{h,s} = \sum_{m=1}^M \frac{1}{M} \theta_m^{h,s}. \quad (11)$$

Following the model aggregation, the server broadcast the updated model back to the clients to for subsequent local training.

5 Experiment

5.1 Dataset Description

Our experiments are conducted on PACS [26], DomainNet [42], and Office-Home [53], each of them consists of several domains. PACS includes 4 distinct domains: Photo (P), Art Painting (A), Cartoon (C), and Sketch (S), each featuring images from 7 common categories. DomainNet encompasses 6 distinct domains: Clipart (C), Infograph (I), Painting (P), Quickdraw (Q), Real (R), and Sketch (S). Initially, each domain comprises 345 classes, but for our study, we narrow this down to 10 commonly used classes to create our experimental dataset. Office-Home contains 4 distinct domains: Art (A), Clipart (C), Product (P), and Real-World (R), each containing 65 classes. We retain all classes within Office-Home to conduct a comprehensive evaluation of DualFed on a larger-scale dataset.

For these datasets, we select the images from a single domain to form the dataset of an individual client. In both PACS and DomainNet, we choose a subset of 500 training images per client from the same domain for the training dataset. For Office-Home, we set the number of training samples to 2,000 for the Clipart, Product, and Real-World domains. In the case of the Art domain, the number is limited to 1,942, matching the total number of samples available in this domain. All the images from the test dataset are reserved for evaluation for these datasets. We apply random flipping and rotational augmentations to these images during the training.

5.2 Compared Methods

We perform a comparative analysis against the following methods, including FedAvg[37], FedProx[28], FedPer[1], FedRep[11], LG-FedAvg[32], FedBN[29], FedProto[51], SphereFed[12], Fed-RoD[6], FedETF[31]. Additionally, the SingleSet method, where separate models are trained and tested for each client using only their private data, is also used for comparison in our experiments.

5.3 Implementation Details

The adopted encoder is from the one of the ResNet18 model pre-trained on the ImageNet dataset [18]. It is followed by a projector network, which consists of an FC network with the architecture: [Linear(512, 256) - ReLU - BN - Linear(256, 512) - BN]. To ensure uniform model capacity, all compared methods employ this Encoder-Projector architecture for representation extraction.

The learning rate is set 0.01, with a momentum of 0.5, for all methods except SphereFed. For SphereFed, we set the learning rate to 1.0 for Office-Home and to 0.1 for both DomainNet and PACS. The batch size is set to 256 for all methods. The epoch of local updating is set to 1 for all methods except FedRep. For FedRep, it has a total of 5 local epochs, with the initial 4 epochs focusing on classifier optimization and the last epoch on encoder and projector optimization. The total global rounds is set to 300.

The other hyperparameters for different methods are selected by grid searching. To mitigate cross-domain interference and potential privacy issues related to BN layers, we localize the *running-mean* and *running-var* components within these layers for all methods.

To ensure the reliability of our results, each experiment is repeated 5 times with random seeds: {0, 1, 2, 3, 4}. The subsequent

sections will detail the mean and standard deviation of the highest test accuracy achieved during FL training.

5.4 Experimental Results

Tables 1 - 3 showcase the experimental results of our proposed DualFed alongside other FL methods on the PACS, Office-Home, and DomainNet datasets, respectively. Notably, DualFed presents a significant performance gain in comparison to these SOTA methods.

Interestingly, the SingleSet model stands out as a strong benchmark, despite not collaborating with other clients, particularly in simpler domains, such as the Quickdraw domain in the DomainNet dataset. The underlying reason is that these simpler domains requires less complex semantic information for downstream tasks. In these cases, a personalized encoder’s representations are sufficient, and collaboration for extensive semantic extraction might be unnecessary or even detrimental. This observation is supported by LG-FedAvg’s performance, which, while also utilizing a personalized encoder for representation extraction, outperforms SingleSet by leveraging collaborative training for a global classifier.

Table 1: Experimental Results on PACS Dataset.

Method	P	A	C	S	Avg.
SingleSet	97.78±0.56	88.12±0.25	89.19±0.37	91.01±0.73	91.52±0.10
FedAvg	97.72±0.56	89.24±1.01	89.32±0.60	91.01±0.70	91.82±0.34
FedProx	97.90±0.38	89.14±1.18	89.40±0.61	91.52±0.72	91.99±0.38
FedPer	98.20±0.42	89.54±1.16	91.28±0.75	91.29±0.60	92.58±0.57
FedRep	97.84±0.35	89.83±1.33	89.96±0.27	91.39±0.48	92.25±0.22
LG-FedAvg	97.60±0.54	88.46±0.45	89.74±0.30	91.36±0.66	91.79±0.24
FedBN	92.20±0.46	89.88±0.86	90.38±0.75	91.34±0.53	92.45±0.37
FedProto	97.90±0.19	91.15±0.50	92.22±0.61	92.99±0.59	93.57±0.34
SphereFed	98.26±0.35	88.95±0.87	91.11±0.42	91.03±0.82	92.34±0.26
Fed-RoD	98.02±0.36	88.85±1.04	89.79±0.49	90.85±0.59	91.88±0.31
FedETF	97.43±0.24	90.95±0.77	90.26±0.29	90.70±0.68	92.33±0.30
DualFed	98.32±0.24	92.47±0.42	94.91±0.63	94.32±0.61	95.01±0.31

Table 2: Experimental Results on Office-Home Dataset.

Method	A	C	P	R	Avg.
SingleSet	66.52±1.27	74.27±0.60	87.46±1.02	77.54±0.58	76.45±0.32
FedAvg	68.82±1.30	74.91±1.02	85.82±0.36	80.30±0.53	77.46±0.35
FedProx	68.78±1.37	74.73±0.79	85.73±0.35	80.25±0.70	77.37±0.33
FedPer	70.31±1.07	75.03±0.38	87.76±0.18	80.51±0.43	78.40±0.40
FedRep	70.23±0.96	75.44±0.69	85.82±0.45	80.39±0.92	77.97±0.37
LG-FedAvg	67.22±1.30	75.33±0.19	87.44±0.43	77.80±0.27	76.94±0.26
FedBN	68.58±1.23	76.01±0.45	86.31±0.96	79.40±0.40	77.58±0.29
FedProto	67.92±0.74	75.76±0.57	87.80±0.30	77.89±0.41	77.34±0.25
SphereFed	66.68±0.89	69.12±0.82	81.92±0.95	76.76±0.28	73.62±0.48
Fed-RoD	68.21±0.86	75.42±0.37	86.40±0.72	80.30±0.79	77.58±0.22
FedETF	69.90±1.14	74.64±0.41	85.52±0.35	80.18±0.39	77.56±0.29
DualFed	71.01±0.71	77.41±0.47	88.84±0.47	81.70±0.28	79.74±0.37

However, as the complexity within a domain increases, such as in the Infograph domain of DomainNet, the benefits of sharing the encoder among clients become apparent. This collaborative approach allows the encoder to extract more nuanced semantic information from the raw data, improving overall model performance, as demonstrated by the results of FedAvg and FedProx. FedRep and FedPer, employing a personalized classifier to adapt the representations from the global encoder, often outperform FedAvg and FedProx. However, these methods primarily leverage the global encoder’s representations and do not fully utilize personalized information to cater to the local data distribution on individual clients.

FedProto significantly improves model performance by aligning representations from different clients within a unified representation space. Nonetheless, this alignment can result in a loss of semantic information pertinent to local tasks due to varying data distributions across clients. This issue is even more pronounced in models like SphereFed and FedETF, which employ a predefined classifier for representation alignment and lack specific semantic information about local data.

Fed-RoD adopts an architecture similar to ours, utilizing both global and personalized classifiers to capture generalized and personalized information. However, it attempts to utilize representations at the same stage, posing challenges in simultaneously meeting these two contradictory objectives. In contrast, our proposed method strategically separates these two conflicting objectives into different stages of the model. This division allows us to achieve both generalization and personalization more effectively, ultimately resulting in superior performance across a wider range of scenarios.

5.5 Additional Analysis

Comparison of global and personalized classifiers. To gain a deeper understanding of the behavior of the global and personalized classifiers, we compare their accuracy, individually and in combination, during training. Figure 3 shows the corresponding experimental results on DomainNet. It is evident that personalized classifier significantly surpasses the global one, owing to its better alignment with local data distributions. Nevertheless, the accuracy of the local classifier can be significantly improved by combining its predictions with those from the global classifier. This enhancement is particularly notable in complex domains, such as Infograph. Conversely, in simpler domains like Quickdraw and Sketch, the benefit of combining classifiers becomes less pronounced. This occurs because, in simpler domains, the representations extracted by the personalized projection network are sufficient for each client’s local tasks, thereby reducing the necessity for more diverse representations from the global encoder.

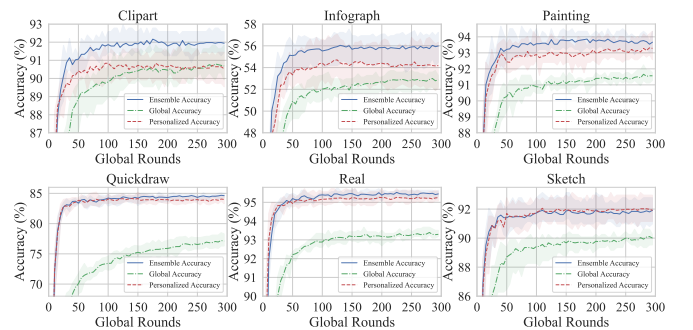
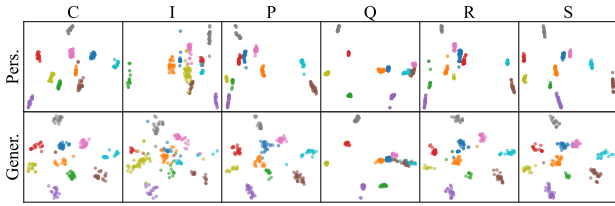


Figure 3: Test accuracy during training on DomainNet.

Visualization of generalized and personalized representations. To intuitively understand the generalized and personalized representations, we utilize t-SNE [52] for visualization. Figure 4 illustrates the visualization of both the generalized and personalized representations on DomainNet dataset. In these visualizations, different colors indicate different classes. It is noticeable that the

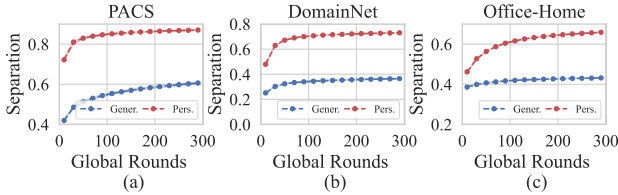
Table 3: Experimental Results on DomainNet Dataset.

Method	C	I	P	Q	R	S	Avg.
SingleSet	88.25±0.81	50.99±1.24	89.60±1.00	82.78±0.43	94.07±0.12	88.16±0.53	82.31±0.19
FedAvg	89.47±0.97	53.70±0.86	89.60±0.52	80.58±0.80	92.85±0.52	88.56±0.58	82.46±0.33
FedProx	89.47±0.86	53.79±0.96	89.56±0.55	80.56±0.87	92.87±0.54	88.63±0.56	82.48±0.38
FedPer	89.70±0.81	54.22±0.68	92.12±0.98	82.18±0.65	94.76±0.41	89.57±0.66	83.76±0.32
FedRep	89.62±0.76	54.19±0.71	90.60±0.37	80.84±0.91	93.03±0.49	89.03±0.77	82.88±0.24
LG-FedAvg	88.56±0.83	51.54±1.18	89.89±0.78	82.68±0.74	94.20±0.32	88.59±0.70	82.58±0.09
FedBN	89.85±0.67	54.58±1.04	91.34±0.90	80.62±0.68	93.76±0.44	89.06±0.41	83.20±0.36
FedProto	90.04±0.86	54.31±0.91	92.18±0.55	84.82±0.67	94.82±0.25	90.40±0.56	84.43±0.30
SphereFed	88.97±0.52	51.02±1.63	90.69±0.43	78.50±1.18	92.65±0.33	88.77±0.54	81.77±0.48
Fed-RoD	89.70±0.99	52.91±0.89	90.18±0.51	81.64±0.50	93.03±0.46	88.88±0.73	82.72±0.25
FedETF	88.97±0.81	55.65±0.85	91.76±0.52	79.76±0.48	94.15±0.23	89.03±0.39	83.22±0.31
DualFed	92.51±0.41	56.77±0.95	94.41±0.30	85.18±0.30	94.69±0.08	92.27±0.54	86.14±0.12

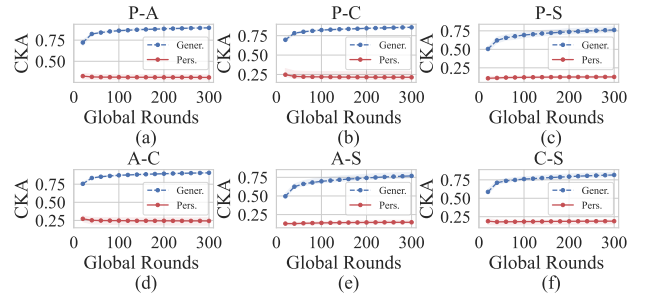
**Figure 4: Visualization of representations on DomainNet.**

personalized representations are more discriminative than the generalized ones, yet they exhibit lower consistency across clients. This demonstrates that DualFed can effectively separate the representation extraction process into two distinct stages, each characterized by high levels of generalization and personalization, respectively.

Quantitative evaluation of generalized and personalized representations. We employ two metrics to quantitatively evaluate the evolution of generalized and personalized representations during training. To quantify the personalization of representations on clients, we adopt the class-wise *separation* in [23]. Additionally, we adopt the *linear centered kernel alignment (CKA)* [24], to measure the generalization ability of representation. Figure 5 presents the varying of *separation* during the training. The personalized representations can achieve higher class separation compared with the generalized representations. However, as shown in Figure 6, the similarity between clients of generalized representations is significant higher than that of the personalized representations.

**Figure 5: Class-wise separation during training.**

Comparison of Training Strategy. DualFed employs a stage-wise training strategy, ensuring that the pre-projection representation remain undisturbed by specific local tasks, thereby maintaining its generalization. Here, we compare this training strategy with the one that training all parameters simultaneously. As shown in Table 4, when E is relatively small (i.e., $E = 1$), simultaneous training can, in fact, outperform stage-wise training. However, as E increases (i.e., $E = 20$), simultaneous training lead to a obvious

**Figure 6: Client-wise CKA similarity during training.**

performance drop in PACS and DomainNet. This trend can be attributed to the fact that an increased number of local epochs causes the pre-projection representations to align more closely with the local task, thereby reducing their generalization.

Table 4: Experiments with Different Training Strategy.

E	Strategy	PACS	DomainNet	Office-Home
1	Stage-wise	95.01±0.31	86.14±0.12	79.74±0.37
	Simu.	95.15±0.16	86.68±0.20	80.57±0.09
20	Stage-wise	94.17±0.28	84.49±0.18	75.93±0.77
	Simu.	93.85±0.30	84.71±0.33	75.42±0.65

Effect of Projector Architecture. We investigate the impact of the architecture of the projection network in three key aspects: the model depth (D), the dimension of hidden layers (H), the impact of BN layers. The corresponding results are shown in Table 5. While increasing D can lead to more generalized pre-projection representations, it simultaneously reduces their discriminative power. Therefore, it is advisable to select an optimal D that maintains a balance in the discriminative and generalized ability of the pre-projection representations. Increasing H can enhance the model performance in most times. The importance of BN layers becomes more pronounced as the scale of the dataset increases.

Effect of Position of Global Classifier. In DualFed, we employ a global classifier for generalized representations and a personalized classifier for personalized representations. Here we conduct experiments when placing the global classifier after the projector. In these experiments, we maintained a shared encoder and investigated two configurations: sharing the projection network (DualFed-G) and personalizing it (DualFed-P). As indicated in Table 6, removing

Table 5: Experiments with Different Projector Architecture.

D	H	BN	PACS	DomainNet	Office-Home
1	256	✓	94.72±0.18	86.16±0.09	79.96±0.24
2	256	✓	95.01±0.31	86.14±0.12	79.74±0.37
3	256	✓	94.97±0.18	85.91±0.26	79.31±0.36
2	64	✓	95.35±0.19	86.06±0.32	79.43±0.24
2	128	✓	95.15±0.18	85.95±0.18	79.49±0.21
2	512	✓	95.21±0.17	86.23±0.23	79.97±0.35
2	256	✗	95.13±0.19	86.23±0.26	79.22±0.38

the global classifier to the same stage as the personalized classifier results in a significant performance decrease. This underscores the importance of the representations at different stages, as they provide complementary information.

Table 6: Experimental Results when Placing Global Classifier at Different Positions.

	PACS	DomainNet	Office-Home
DualFed	95.01±0.31	86.14±0.12	79.74±0.37
DualFed-P	94.95±0.18	85.55±0.09	78.24±0.29
DualFed-G	94.84±0.12	84.90±0.42	78.08±0.17

Effect of Personalized Layers. Table 7 presents the model performance with different personalization strategy. The results indicate that combining a global encoder with a personalized projection network significantly enhances model performance, as it integrates both generalized and personalized information.

Table 7: Experimental Results with Different Parameter Personalized Strategies, where ✓ Denotes the Personalized Parameters, ✗ Denotes the Global Parameters.

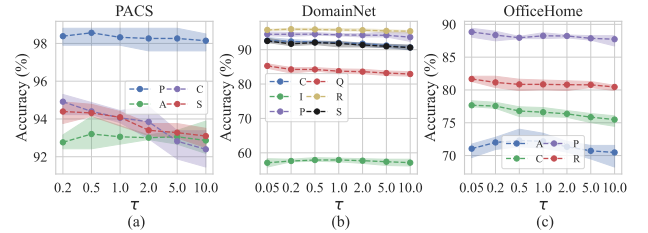
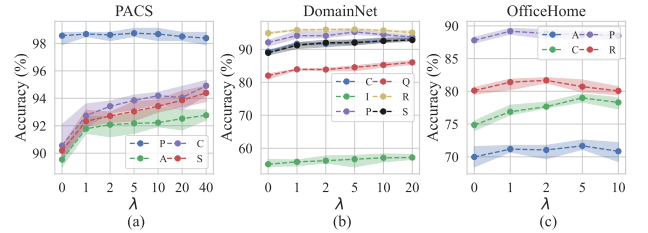
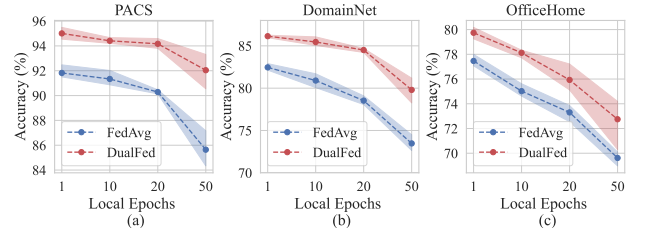
Enc.	Prj.	P.C.	G.C.	PACS	DomainNet	Office-Home
✗	✓	✓	✓	94.96±0.26	86.16±0.27	79.33±0.41
✗	✓	✓	✗	95.01±0.31	86.11±0.19	79.74±0.28
✗	✗	✗	✗	94.58±0.22	84.55±0.30	78.58±0.46
✗	✗	✓	✗	94.80±0.20	85.21±0.16	79.19±0.19
✓	✓	✓	✓	93.73±0.08	83.50±0.43	77.85±0.44

Communication Costs. We assess the communication costs by using the total number of model parameters transferred to reach a predefined target accuracy during training. For PACS, DomainNet, and Office-Home, the target accuracies are set to 85%, 75%, and 70%, respectively. As illustrated in Table 8, DualFed outperforms other methods by achieving the same target accuracy with lower communication costs, showcasing its practical efficiency.

Effect of Hyper Parameters. We conduct experiments using various hyperparameters, including the temperature coefficient (τ), the loss balance coefficient (λ), and the number of local epochs (E). As depicted in Figure 7, we observe that as τ increases, its effectiveness in distinguishing between different classes diminishes, thereby losing the advantage of contrastive loss. Figure 8 presents the test accuracy with varying λ . Setting λ to 0 is equivalent to training the model solely with cross-entropy loss. Increasing λ enhances the distinctiveness and relevance of personalized representations to the local task, which, in turn, improves model performance. Figure 9 shows the test accuracy with different local epochs, it illustrates

Table 8: Averaged Communication Costs (MB) when Reaching the Same Target Accuracy during Training.

	PACS	DomainNet	Office-Home
FedAvg	1920.93	2008.52	2538.72
FedProx	1833.62	2008.52	2538.72
FedPer	1658.47	1658.47	2007.62
FedRep	2705.92	3316.94	3753.37
FedBN	1482.91	1832.08	2098.97
SphereFed	3142.36	5586.42	18330.43
Fed-RoD	1135.10	1309.90	1663.30
FedETF	11783.85	15537.22	15973.66
DualFed	611.21	873.27	1225.59

**Figure 7: Test accuracy with varying temperature coefficient.****Figure 8: Test accuracy with varying loss balance coefficient.****Figure 9: Test accuracy with varying local epochs.**

that DualFed consistently surpasses FedAvg across various local epochs, demonstrating its robustness to local epochs.

6 Conclusion

In this paper, we propose a new PFL approach called DualFed. It decouples the objectives of generalization and personalization in PFL by a personalized projection network. This modification reduces the mutual interference between the conflicting optimization objectives in traditional PFL, thereby achieving a win-win situation of both generalization and personalization in PFL. Our experiments across various datasets have shown the effectiveness of DualFed.

Acknowledgment

This work was supported by the National Natural Science Foundation of China under Grants 62372028 and 62372027.

References

- [1] Manoj Guhan Arivazhagan, Vinay Aggarwal, Aaditya Kumar Singh, and Sunav Choudhary. 2019. Federated learning with personalization layers. *arXiv preprint arXiv:1912.00818* (2019).
- [2] Florian Bordes, Randall Balestriero, Quentin Garrido, Adrien Bardes, and Pascal Vincent. 2023. Guillotine Regularization: Why removing layers is needed to improve generalization in Self-Supervised Learning. *Transactions on Machine Learning Research* (2023).
- [3] Luxin Cai, Naiyue Chen, Yuanzhouhan Cao, Jiahuan He, and Yidong Li. 2023. FedCE: Personalized Federated Learning Method based on Clustering Ensembles. In *Proceedings of the 31st ACM International Conference on Multimedia*. 1625–1633.
- [4] Debora Caldarola, Massimiliano Mancini, Fabio Galasso, Marco Ciccone, Emanuele Rodolà, and Barbara Caputo. 2021. Cluster-driven graph federated learning over multiple domains. In *Proceedings of the IEEE/CVF Conference on Computer Vision and Pattern Recognition*. 2749–2758.
- [5] Mathilde Caron, Ishan Misra, Julien Mairal, Priya Goyal, Piotr Bojanowski, and Armand Joulin. 2020. Unsupervised learning of visual features by contrasting cluster assignments. *Advances in neural information processing systems* 33 (2020), 9912–9924.
- [6] Hong-You Chen and Wei-Lun Chao. 2022. On Bridging Generic and Personalized Federated Learning for Image Classification. In *International Conference on Learning Representations*.
- [7] Mingkan Chen, Jingtao Sun, Kento Aida, and Atsuko Takefusa. 2024. Weather-aware object detection method for maritime surveillance systems. *Future Generation Computer Systems* 151 (2024), 111–123.
- [8] Ting Chen, Simon Kornblith, Mohammad Norouzi, and Geoffrey Hinton. 2020. A simple framework for contrastive learning of visual representations. In *International conference on machine learning*. PMLR, 1597–1607.
- [9] Xinlei Chen, Haoqi Fan, Ross Girshick, and Kaiming He. 2020. Improved baselines with momentum contrastive learning. *arXiv preprint arXiv:2003.04297* (2020).
- [10] Xinlei Chen and Kaiming He. 2021. Exploring simple siamese representation learning. In *Proceedings of the IEEE/CVF conference on computer vision and pattern recognition*. 15750–15758.
- [11] Liam Collins, Hamed Hassani, Aryan Mokhtari, and Sanjay Shakkottai. 2021. Exploiting shared representations for personalized federated learning. In *International Conference on Machine Learning*. PMLR, 2089–2099.
- [12] Xin Dong, Sai Qian Zhang, Ang Li, and HT Kung. 2022. Sphered: Hyperspherical federated learning. In *European Conference on Computer Vision*. Springer, 165–184.
- [13] Yutong Feng, Jianwen Jiang, Mingqian Tang, Rong Jin, and Yue Gao. 2021. Re-thinking Supervised Pre-training for Better Downstream Transferring. *arXiv e-prints* (2021), arXiv–2110.
- [14] Avishek Ghosh, Jichan Chung, Dong Yin, and Kannan Ramchandran. 2020. An efficient framework for clustered federated learning. *Advances in Neural Information Processing Systems* 33 (2020), 19586–19597.
- [15] Jean-Bastien Grill, Florian Strub, Florent Altché, Corentin Tallec, Pierre Richemond, Elena Buchatskaya, Carl Doersch, Bernardo Avila Pires, Zhaohan Guo, Mohammad Gheshlaghi Azar, et al. 2020. Bootstrap your own latent: a new approach to self-supervised learning. *Advances in neural information processing systems* 33 (2020), 21271–21284.
- [16] Yu Gui, Cong Ma, and Yiqiao Zhong. 2023. Unraveling Projection Heads in Contrastive Learning: Insights from Expansion and Shrinkage. *arXiv preprint arXiv:2306.03335* (2023).
- [17] Mahmoud Hassaballah, Mourad A Kenk, Khan Muhammad, and Shervin Minaee. 2020. Vehicle detection and tracking in adverse weather using a deep learning framework. *IEEE transactions on intelligent transportation systems* 22, 7 (2020), 4230–4242.
- [18] Kaiming He, Xiangyu Zhang, Shaoqing Ren, and Jian Sun. 2016. Deep residual learning for image recognition. In *Proceedings of the IEEE conference on computer vision and pattern recognition*. 770–778.
- [19] Li Jing, Pascal Vincent, Yann LeCun, and Yuandong Tian. 2022. UNDERSTANDING DIMENSIONAL COLLAPSE IN CONTRASTIVE SELF-SUPERVISED LEARNING. In *10th International Conference on Learning Representations, ICLR 2022*.
- [20] Peter Kairouz, H Brendan McMahan, Brendan Avent, Aurélien Bellet, Mehdi Bennis, Arjun Nitin Bhagoji, Kallista Bonawitz, Zachary Charles, Graham Cormode, Rachel Cummings, et al. 2021. Advances and open problems in federated learning. *Foundations and Trends® in Machine Learning* 14, 1–2 (2021), 1–210.
- [21] Sai Praneeth Karimireddy, Satyen Kale, Mehryar Mohri, Sashank Reddi, Sebastian Stich, and Ananda Theertha Suresh. 2020. Scaffold: Stochastic controlled averaging for federated learning. In *International conference on machine learning*. PMLR, 5132–5143.
- [22] Prannay Khosla, Piotr Teterwak, Chen Wang, Aaron Sarna, Yonglong Tian, Phillip Isola, Aaron Maschinot, Ce Liu, and Dilip Krishnan. 2020. Supervised contrastive learning. *Advances in neural information processing systems* 33 (2020), 18661–18673.
- [23] Simon Kornblith, Ting Chen, Honglak Lee, and Mohammad Norouzi. 2021. Why do better loss functions lead to less transferable features? *Advances in Neural Information Processing Systems* 34 (2021), 28648–28662.
- [24] Simon Kornblith, Mohammad Norouzi, Honglak Lee, and Geoffrey Hinton. 2019. Similarity of neural network representations revisited. In *International conference on machine learning*. PMLR, 3519–3529.
- [25] Sam Leroux, Bo Li, and Pieter Simoons. 2022. Multi-branch neural networks for video anomaly detection in adverse lighting and weather conditions. In *Proceedings of the IEEE/CVF Winter Conference on Applications of Computer Vision*. 2358–2366.
- [26] Da Li, Yongxin Yang, Yi-Zhe Song, and Timothy M Hospedales. 2017. Deeper, broader and artier domain generalization. In *Proceedings of the IEEE international conference on computer vision*. 5542–5550.
- [27] Tian Li, Anit Kumar Sahu, Ameet Talwalkar, and Virginia Smith. 2020. Federated learning: Challenges, methods, and future directions. *IEEE signal processing magazine* 37, 3 (2020), 50–60.
- [28] Tian Li, Anit Kumar Sahu, Manzil Zaheer, Maziar Sanjabi, Ameet Talwalkar, and Virginia Smith. 2020. Federated optimization in heterogeneous networks. *Proceedings of Machine Learning and systems* 2 (2020), 429–450.
- [29] Xiaoxiao Li, Meirui JIANG, Xiaofei Zhang, Michael Kamp, and Qi Dou. 2021. FedBN: Federated Learning on Non-IID Features via Local Batch Normalization. In *International Conference on Learning Representations*.
- [30] Xiao Li, Sheng Liu, Jinxin Zhou, Xinyu Lu, Carlos Fernandez-Granda, Zhihui Zhu, and Qing Qu. 2022. Principled and efficient transfer learning of deep models via neural collapse. *arXiv preprint arXiv:2212.12206* (2022).
- [31] Zexi Li, Xinyi Shang, Rui He, Tao Lin, and Chao Wu. 2023. No Fear of Classifier Biases: Neural Collapse Inspired Federated Learning with Synthetic and Fixed Classifier. In *Proceedings of the IEEE/CVF International Conference on Computer Vision (ICCV)*. 5319–5329.
- [32] Paul Pu Liang, Terrance Liu, Liu Ziyin, Nicholas B Allen, Randy P Auerbach, David Brent, Ruslan Salakhutdinov, and Louis-Philippe Morency. 2020. Think locally, act globally: Federated learning with local and global representations. *arXiv preprint arXiv:2001.01523* (2020).
- [33] Tsung-Yi Lin, Piotr Dollár, Ross Girshick, Kaiming He, Bharath Hariharan, and Serge Belongie. 2017. Feature pyramid networks for object detection. In *Proceedings of the IEEE conference on computer vision and pattern recognition*. 2117–2125.
- [34] Yunfei Long, Zhe Xue, Lingyang Chu, Tianlong Zhang, Junjiang Wu, Yu Zang, and Junping Du. 2023. Fedcd: A classifier debiased federated learning framework for non-iid data. In *Proceedings of the 31st ACM International Conference on Multimedia*. 8994–9002.
- [35] Mi Luo, Fei Chen, Dapeng Hu, Yifan Zhang, Jian Liang, and Jiashi Feng. 2021. No fear of heterogeneity: Classifier calibration for federated learning with non-iid data. *Advances in Neural Information Processing Systems* 34 (2021), 5972–5984.
- [36] Wojciech Masarczyk, Mateusz Ostaszewski, Ehsan Imani, Razvan Pascanu, Piotr Miłoś, and Tomasz Trzcinski. 2024. The tunnel effect: Building data representations in deep neural networks. *Advances in Neural Information Processing Systems* 36 (2024).
- [37] Brendan McMahan, Eider Moore, Daniel Ramage, Seth Hampson, and Blaise Agüera y Arcas. 2017. Communication-efficient learning of deep networks from decentralized data. In *Artificial intelligence and statistics*. PMLR, 1273–1282.
- [38] Quanzheng Mou, Longsheng Wei, Conghao Wang, Dapeng Luo, Songze He, Jing Zhang, Huimin Xu, Chen Luo, and Changxin Gao. 2021. Unsupervised domain-adaptive scene-specific pedestrian detection for static video surveillance. *Pattern Recognition* 118 (2021), 108038.
- [39] Jaehoon Oh, SangMook Kim, and Se-Young Yun. 2022. FedBABU: Toward Enhanced Representation for Federated Image Classification. In *International Conference on Learning Representations*.
- [40] Chris Olah, Alexander Mordvintsev, and Ludwig Schubert. 2017. Feature visualization. *Distill* 2, 11 (2017), e7.
- [41] Adam Paszke, Sam Gross, Francisco Massa, Adam Lerer, James Bradbury, Gregory Chanan, Trevor Killeen, Zeming Lin, Natalia Gimelshein, Luca Antiga, et al. 2019. Pytorch: An imperative style, high-performance deep learning library. *Advances in neural information processing systems* 32 (2019).
- [42] Xingchao Peng, Qinxun Bai, Xide Xia, Zijun Huang, Kate Saenko, and Bo Wang. 2019. Moment matching for multi-source domain adaptation. In *Proceedings of the IEEE/CVF international conference on computer vision*. 1406–1415.
- [43] Zhuang Qi, Lei Meng, Zitan Chen, Han Hu, Hui Lin, and Xiangxu Meng. 2023. Cross-Silo Prototypical Calibration for Federated Learning with Non-IID Data. In *Proceedings of the 31st ACM International Conference on Multimedia*. 3099–3107.
- [44] Stefano Recanatani, Matthew Farrell, Madhu Advani, Timothy Moore, Guillaume Lajoie, and Eric Shea-Brown. 2019. Dimensionality compression and expansion in deep neural networks. *arXiv preprint arXiv:1906.00443* (2019).
- [45] Mert Bulent Sariyildiz, Yannis Kalantidis, Kartek Alahari, and Diane Larlus. 2023. No Reason for No Supervision: Improved Generalization in Supervised Models.

- In *ICLR 2023-International Conference on Learning Representations*. 1–26.
- [46] Felix Sattler, Klaus-Robert Müller, and Wojciech Samek. 2020. Clustered federated learning: Model-agnostic distributed multitask optimization under privacy constraints. *IEEE transactions on neural networks and learning systems* 32, 8 (2020), 3710–3722.
- [47] Yiqing Shen, Yuyin Zhou, and Lequan Yu. 2022. Cd2-pfed: Cyclic distillation-guided channel decoupling for model personalization in federated learning. In *Proceedings of the IEEE/CVF Conference on Computer Vision and Pattern Recognition*. 10041–10050.
- [48] Ravid Shwartz-Ziv and Naftali Tishby. 2017. Opening the black box of deep neural networks via information. *arXiv preprint arXiv:1703.00810* (2017).
- [49] Benyuan Sun, Hongxing Huo, Yi Yang, and Bo Bai. 2021. Partialfed: Cross-domain personalized federated learning via partial initialization. *Advances in Neural Information Processing Systems* 34 (2021), 23309–23320.
- [50] Alysia Ziyang Tan, Han Yu, Lizhen Cui, and Qiang Yang. 2022. Towards personalized federated learning. *IEEE Transactions on Neural Networks and Learning Systems* (2022).
- [51] Yue Tan, Guodong Long, Lu Liu, Tianyi Zhou, Qinghua Lu, Jing Jiang, and Chengqi Zhang. 2022. Fedproto: Federated prototype learning across heterogeneous clients. In *Proceedings of the AAAI Conference on Artificial Intelligence*, Vol. 36. 8432–8440.
- [52] Laurens Van der Maaten and Geoffrey Hinton. 2008. Visualizing data using t-SNE. *Journal of machine learning research* 9, 11 (2008).
- [53] Hemanth Venkateswara, Jose Eusebio, Shayok Chakraborty, and Sethuraman Panchanathan. 2017. Deep hashing network for unsupervised domain adaptation. In *Proceedings of the IEEE conference on computer vision and pattern recognition*. 5018–5027.
- [54] Peng Wang, Xiao Li, Can Yaras, Zhihui Zhu, Laura Balzano, Wei Hu, and Qing Qu. 2023. Understanding Deep Representation Learning via Layerwise Feature Compression and Discrimination. *arXiv preprint arXiv:2311.02960* (2023).
- [55] Yizhou Wang, Shixiang Tang, Feng Zhu, Lei Bai, Rui Zhao, Donglian Qi, and Wanli Ouyang. 2022. Revisiting the transferability of supervised pretraining: an mlp perspective. In *Proceedings of the IEEE/CVF Conference on Computer Vision and Pattern Recognition*. 9183–9193.
- [56] Xinghao Wu, Xuefeng Liu, Jianwei Niu, Haolin Wang, Shaojie Tang, Guogang Zhu, and Hao Su. 2024. Decoupling General and Personalized Knowledge in Federated Learning via Additive and Low-Rank Decomposition. *arXiv preprint arXiv:2406.19931* (2024).
- [57] Xinghao Wu, Xuefeng Liu, Jianwei Niu, Guogang Zhu, and Shaojie Tang. 2023. Bold but cautious: Unlocking the potential of personalized federated learning through cautiously aggressive collaboration. In *Proceedings of the IEEE/CVF International Conference on Computer Vision*. 19375–19384.
- [58] Xinghao Wu, Xuefeng Liu, Jianwei Niu, Guogang Zhu, Shaojie Tang, Xiaotian Li, and Jiannong Cao. 2024. The Diversity Bonus: Learning from Dissimilar Distributed Clients in Personalized Federated Learning. arXiv:2407.15464 [cs.LG] <https://arxiv.org/abs/2407.15464>
- [59] Yihao Xue, Eric Gan, Jiayi Ni, Siddharth Joshi, and Baharan Mirzasoileman. 2024. Investigating the Benefits of Projection Head for Representation Learning. *arXiv preprint arXiv:2403.11391* (2024).
- [60] Fu-En Yang, Chien-Yi Wang, and Yu-Chiang Frank Wang. 2023. Efficient model personalization in federated learning via client-specific prompt generation. In *Proceedings of the IEEE/CVF International Conference on Computer Vision*. 19159–19168.
- [61] Jason Yosinski, Jeff Clune, Yoshua Bengio, and Hod Lipson. 2014. How transferable are features in deep neural networks? *Advances in neural information processing systems* 27 (2014).
- [62] Jure Zbontar, Li Jing, Ishan Misra, Yann LeCun, and Stéphane Deny. 2021. Barlow twins: Self-supervised learning via redundancy reduction. In *International conference on machine learning*. PMLR, 12310–12320.
- [63] Matthew D Zeiler and Rob Fergus. 2014. Visualizing and understanding convolutional networks. In *Computer Vision—ECCV 2014: 13th European Conference, Zurich, Switzerland, September 6–12, 2014, Proceedings, Part I 13*. Springer, 818–833.
- [64] Jianqing Zhang, Yang Hua, Hao Wang, Tao Song, Zhengui Xue, Ruhui Ma, Jian Cao, and Haibing Guan. 2023. Gpfl: Simultaneously learning global and personalized feature information for personalized federated learning. In *Proceedings of the IEEE/CVF International Conference on Computer Vision*. 5041–5051.
- [65] Jianqing Zhang, Yang Hua, Hao Wang, Tao Song, Zhengui Xue, Ruhui Ma, and Haibing Guan. 2023. Fedcp: Separating feature information for personalized federated learning via conditional policy. In *Proceedings of the 29th ACM SIGKDD Conference on Knowledge Discovery and Data Mining*. 3249–3261.
- [66] Yue Zhao, Meng Li, Liangzhen Lai, Naveen Suda, Damon Civin, and Vikas Chandr. 2018. Federated learning with non-iid data. *arXiv preprint arXiv:1806.00582* (2018).
- [67] Kaiyu Zheng, Xuefeng Liu, Guogang Zhu, Xinghao Wu, and Jianwei Niu. 2022. Channelfed: Enabling personalized federated learning via localized channel attention. In *GLOBECOM 2022-2022 IEEE Global Communications Conference*. IEEE, 2987–2992.
- [68] Tailin Zhou, Jun Zhang, and Danny HK Tsang. 2023. FedFA: Federated Learning with Feature Anchors to Align Features and Classifiers for Heterogeneous Data. *IEEE Transactions on Mobile Computing* (2023).
- [69] Guogang Zhu, Xuefeng Liu, Shaojie Tang, and Jianwei Niu. 2022. Aligning before aggregating: Enabling cross-domain federated learning via consistent feature extraction. In *2022 IEEE 42nd International Conference on Distributed Computing Systems (ICDCS)*. IEEE, 809–819.
- [70] Guogang Zhu, Xuefeng Liu, Shaojie Tang, and Jianwei Niu. 2023. Aligning before Aggregating: Enabling Communication Efficient Cross-Domain Federated Learning via Consistent Feature Extraction. *IEEE Transactions on Mobile Computing* (2023).
- [71] Guogang Zhu, Xuefeng Liu, Shaojie Tang, Jianwei Niu, Xinghao Wu, and Jiaying Shen. 2023. Take Your Pick: Enabling Effective Personalized Federated Learning within Low-dimensional Feature Space. *arXiv preprint arXiv:2307.13995* (2023).
- [72] Hangyu Zhu, Jinjin Xu, Shiqing Liu, and Yaochu Jin. 2021. Federated learning on non-IID data: A survey. *Neurocomputing* 465 (2021), 371–390.

Supplementary Materials - DualFed: Enjoying both Generalization and Personalization in Federated Learning via Hierarchical Representations

1 Algorithm Details for DualFed

The training procedure for DualFed is presented in Algorithm 1. It mainly consists of the following steps within a single global round:

- The sever sends a global encoder and classifier to each client.
- Each client loads the parameters from the received global encoder and classifier into its local ones, then iteratively updates the main branch (including the global encoder, the personalized projector, and the personalized classifier) and the global classifier using its local data.
- Once local updating is completed, each client uploads its latest global encoder and classifier to the server.
- The sever aggregates these uploaded global encoder and classifier to generate the new ones.

The above steps are repeated until the model converges.

2 Dataset Description

Our experiments are conducted on three datasets: PACS [8], DomainNet [15], and Office-Home [17]. The PACS dataset includes 4 distinct domains: Photo (P), Art (A), Cartoon (C), and Sketch (S), each containing images from 7 common classes. The DomainNet dataset encompasses 6 distinct domains: Clipart (C), Infograph (I), Painting (P), Quickdraw (Q), Real (R), and Sketch (S). Initially, each domain in DomainNet dataset comprises 345 classes. Following previous studies [10, 18], we narrow these domains down to 10 commonly-used classes to create our experimental dataset. The Office-Home dataset contains images from 4 distinct domains: Art (A), Clipart (C), Product (P), and Real-World (R), each containing 65 classes. We retain all classes in Office-Home to conduct a comprehensive evaluation of DualFed on a larger-scale scenario. Figure 1 presents some example images in these three datasets. For each domain, we show the images from 5 representing classes. It can be observed that significant variations exist among different domains, suggesting that personalized representations can vary considerably across these domains. Therefore, it is crucial to explore both generalized representations shared across these domains and personalized representations specific to each domain to enhance collaboration in federated learning (FL) with heterogenous data.

For these three datasets, we select the images from a single domain to form the dataset of an individual client. Consequently, there are 4 clients for PACS, 6 clients for DomainNet, and 4 clients for Office-Home, respectively. In both PACS and DomainNet datasets, we chose a subset of 500 training images per client from the same domain to comprise the training dataset. For Office-Home dataset, we consider a more extensive experimental scenario with more samples. We set the number of training samples to 2,000 for the Clipart, Product, and Real-World domains. In the case of the Art domain, the number is limited to 1,942, matching the total number of samples available in this domain. All the images from the test dataset are reserved for evaluation for these datasets. In line with

Algorithm 1 DualFed

Notations: T : global updating rounds, E : local updating epochs, B : local minibatch size, η : learning rate, λ : loss-balanced hyperparameters, $\theta_m^{f,s,t}$: parameters of global encoder, $\theta_m^{h,s,t}$: parameters of global classifier, $\theta_m^{g,p,t}$: parameters of personalized projection network, $\theta_m^{h,p,t}$: parameters of personalized classifier, $\Theta_m^t := \{\theta_m^{f,s,t}, \theta_m^{h,s,t}, \theta_m^{g,p,t}, \theta_m^{h,p,t}\}$: parameters of local model, $\bar{\Theta}_m^t := \{\theta_m^{f,s,t}, \theta_m^{g,p,t}, \theta_m^{h,p,t}\}$: parameters of main branch, $\tilde{\theta}^{f,s,t}$: aggregated parameters of global encoder, $\tilde{\theta}^{h,s,t}$: aggregated parameters of global classifier.

Sever Executes:

```

1: # model initialization
2: broadcast initialized model  $\Theta^1$  to each client
3: for  $t = 1, 2, 3, \dots, T$  do
4:   # performing local updating
5:   for each client  $m$  in parallel do
6:      $\theta_m^{f,s,t+1}, \theta_m^{h,s,t+1} \leftarrow \text{ClientUpdate}(m, t, \tilde{\theta}^{f,s,t}, \tilde{\theta}^{h,s,t})$ 
7:   end for
8:   # aggregating global encoder and classifier
9:    $\tilde{\theta}^{f,s,t+1} = \sum_{m=1}^M \frac{1}{M} \theta_m^{f,s,t+1}$ ,  $\tilde{\theta}^{h,s,t+1} = \sum_{m=1}^M \frac{1}{M} \theta_m^{h,s,t+1}$ 
10: end for
11: ClientUpdate( $m, t, \tilde{\theta}^{f,s,t}, \tilde{\theta}^{h,s,t}$ ):
12: # loading global encoder and classifier
13:  $\theta_m^{f,s,t} \leftarrow \tilde{\theta}^{f,s,t}$ ,  $\theta_m^{h,s,t} \leftarrow \tilde{\theta}^{h,s,t}$ 
14: # updating main branch
15:  $\mathcal{B} \leftarrow$  (split local dataset into batches of size B)
16: for  $i = 1, 2, 3, \dots, E$  do
17:   for batch  $(x_b, y_b) \in \mathcal{B}$  do
18:      $z = f(x_b; \theta_m^{f,s,t})$ ,  $u = f(z; \theta_m^{g,p,t})$ ,  $\hat{y}^p = f(u; \theta_m^{h,p,t})$ 
19:      $\bar{\Theta}_m^t \leftarrow \bar{\Theta}_m^t - \eta \nabla_{\bar{\Theta}_m^t} \mathcal{L}_{pcls}(\hat{y}^p, y_b) + \lambda \mathcal{L}_{con}(u)$ 
20:   end for
21: end for
22: # updating global classifier
23:  $\mathcal{B} \leftarrow$  (split local dataset into batches of size B)
24: for  $i = 1, 2, 3, \dots, E$  do
25:   for batch  $(x_b, y_b) \in \mathcal{B}$  do
26:      $z = f(x_b; \theta_m^{f,s,t})$ ,  $\hat{y}^s = f(z; \theta_m^{h,s,t})$ 
27:      $\theta_m^{h,s,t} \leftarrow \theta_m^{h,s,t} - \eta \nabla_{\theta_m^{h,s,t}} \mathcal{L}_{scfs}(\hat{y}^s, y_b)$ 
28:   end for
29: end for
30:  $\theta_m^{g,p,t+1} \leftarrow \theta_m^{g,p,t}$ ,  $\theta_m^{h,p,t+1} \leftarrow \theta_m^{h,p,t}$ 
31: return  $\theta_m^{f,s,t+1}, \theta_m^{h,s,t+1}$  to server

```

the experimental settings of previous studies, the images are resized to 256×256 for DomainNet, 227×227 for PACS, and 224×224

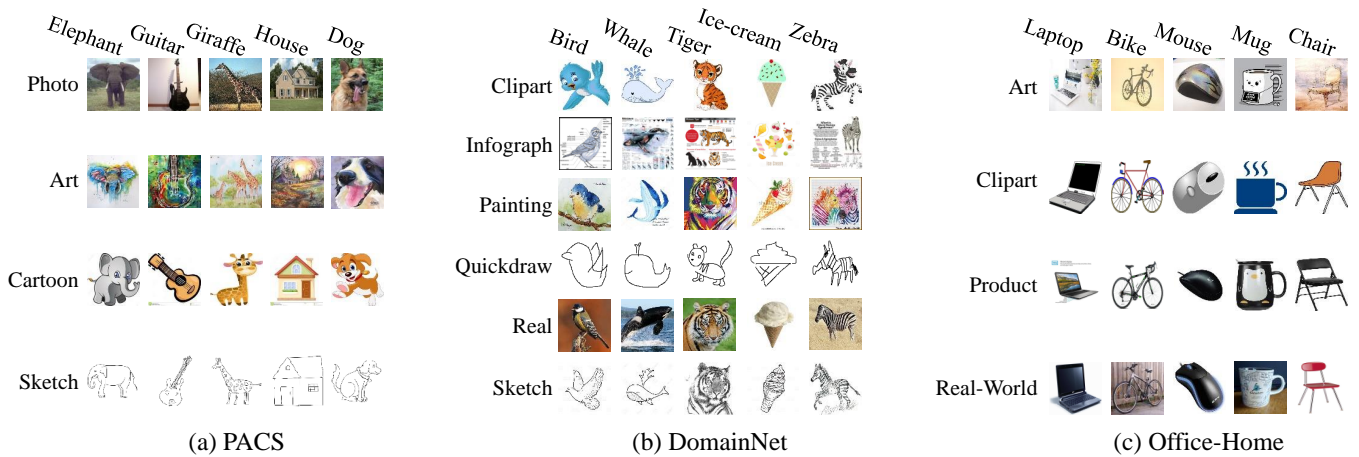


Figure 1: Visualization of example images in the adopted dataset, (a) PACS, (b) DomainNet, (c) Office-Home. We present images from 5 classes for each domain in these datasets.

for Office-Home, respectively, before feeding into the model. Additionally, we apply random flipping and rotational augmentations to these images during the training.

3 Implementation Details of Experiments

In our experiments, we compare DualFed with multiple benchmark FL methods, including FedAvg[13], FedProx[9], FedPer[1], FedRep[3], LG-FedAvg[12], FedBN[10], FedProto[16], SphereFed[4], Fed-RoD[2], FedETF[11]. Additionally, the SingleSet method, where separate models are trained and tested for each client using only their private data, is also used for comparison in our experiments. We reproduce these FL methods based on the discussions in their original paper and the official code^{1,2,3,4,5}, when available.

We modify the ResNet18 model, originally pretrained on the ImageNet dataset, by removing its final fully connected (FC) layer, thereby transforming it into an encoder [5]. This encoder is followed by a projector network, which consists of an FC network with the architecture: [Linear(512, 256) - ReLU - BN - Linear(256, 512) - BN]. To ensure uniform model capacity, all compared methods employ this Encoder-Projector architecture for representation extraction, with only specific alterations made to the classifiers in some approaches. Specifically, SphereFed initializes its classifier orthogonally and maintains it unchanged throughout the training process. In FedETF, the classifier is initialized as an ETF (Equiangular Tight Frame) architecture and kept fixed during the training. FedRoD employs both global and personalized classifiers simultaneously during training. All classifiers utilized in our experiments consist of an FC layer, with 512 input neurons and a number of output neurons that matches the class count.

We conduct all experiments on a Nvidia V100 four-card cluster, utilizing the PyTorch [14] framework. The model is optimized by stochastic gradient descent (SGD) with momentum. The learning

rate is consistently set at 0.01, with a momentum of 0.5, applicable to all methods except SphereFed. Due to the differing loss value magnitudes in SphereFed compared to other methods [4], we carefully adjust its learning rates for each dataset. Consequently, we set the learning rate to 1.0 for Office-Home and to 0.1 for both DomainNet and PACS. During local updates, a batch size of 256 is consistent across all methods. The epoch of local updating is set to 1 for all methods except FedRep. For FedRep, it has a total of 5 local epochs, with the initial 4 epochs focusing on classifier optimization and the last epoch on encoder and projector optimization. The total count of global rounds is set to 300 for all methods.

In our experiments with FedProx, we set the hyperparameter μ —responsible for balancing the loss terms—to 0.01 for all datasets. After extensive searching, we set the hyperparameter for aligning global and local prototypes in FedProto to 1.0 across all datasets. For DualFed, the temperature for representation contrastive learning is set to 0.2 for PACS, and 0.05 for DomainNet and OfficeHome. The λ used to balance the cross entropy loss and contrastive loss is set to 40, 10 and 2 for PACS, DomainNet, and Office-Home, respectively.

To mitigate cross-domain interference and potential privacy issues related to batch normalization (BN) layers, we localize the *running-mean* and *running-var* components within these layers for all methods.

The stage of model evaluation, a critical factor for comparison, is determined based on the settings described in the original papers of the compared FL methods. For FedETF, the model is evaluated after local finetuning on each client. According to its official source code⁵, the global model in FedETF is finetuned for 1 round firstly, then the ETF classifier and projection network are alternately finetuned for 20 rounds. In each of alternative finetuned rounds, both the ETF classifier and projection layer are finetuned for 3 rounds. Apart from FedETF, all other methods undergo evaluation post model aggregation. It should be noted that although SphereFed proposes to conduct model evaluation after the fast federated calibration (FFC), we find this operation is harmful to the model in our settings and report the accuracy after the model aggregation.

¹<https://github.com/litian96/FedProx>

²<https://github.com/med-air/FedBN>

³<https://github.com/yuetan031/FedProto>

⁴<https://github.com/hongyouc/Fed-RoD>

⁵<https://github.com/ZexiLee/ICCV-2023-FedETF>

Table 1: Experiments with Different Projector Architecture.

D	H	BN	Detailed Architecture	PACS	DomainNet	Office-Home
1	256	✓	[Linear(512, 512) - BN]	94.72±0.18	86.16±0.09	79.96±0.24
2	256	✓	[Linear(512, 256) - ReLU - BN - Linear(256, 512) - BN]	95.01±0.31	86.14±0.12	79.74±0.37
3	256	✓	[Linear(512, 256) - ReLU - BN - Linear(256, 256) - ReLU - BN - Linear(256, 512) - BN]	94.97±0.18	85.91±0.26	79.31±0.36
2	64	✓	[Linear(512, 64) - ReLU - BN - Linear(64, 512) - BN]	95.35±0.19	86.06±0.32	79.43±0.24
2	128	✓	[Linear(512, 128) - ReLU - BN - Linear(128, 512) - BN]	95.15±0.18	85.95±0.18	79.49±0.21
2	512	✓	[Linear(512, 512) - ReLU - BN - Linear(512, 512) - BN]	95.21±0.17	86.23±0.23	79.97±0.35
2	256	✗	[Linear(512, 256) - ReLU - Linear(256, 512)]	95.13±0.19	86.23±0.26	79.22±0.38

During the experiments, we choose the accuracy on the test dataset as the metric to quantifying the model performance. To ensure the reliability of our results, each experiment is repeated 5 times with different random seeds: {0, 1, 2, 3, 4}. We report the mean and standard deviation of the highest test accuracy achieved during FL training for all methods.

4 Additional Analysis of DualFed

4.1 Effect of Projection Network Architecture

We investigate the impact of the architecture of the projection network in three key aspects: the depth of projection network (D), the dimension of hidden layers (H), the impact of BN layers. In the experiments, we set D to {1, 2, 3} and H to {64, 128, 256, 512}, respectively. The detailed architecture of projectioion network and the corresponding results are shown in Table 1. From Table 1, we can derive the following conclusions. While increasing D can lead to more generalized pre-projection representations, it simultaneously reduces their discriminative power. Therefore, it is advisable to select an optimal D that maintains a balance in the discriminative and generalized ability of the pre-projection representations. Increasing H can enhance the model performance in most times, as it enables the task-relevant information within the post-projection representations to be effectively passed to the pre-projection representations. The importance of BN layers becomes more pronounced as the scale of the dataset increases.

4.2 Quantitative evaluation of representations

We employ two metrics to quantitatively evaluate the evolution of generalized and personalized representations during training. To quantify the generalization of representations, we adopt the *linear centered kernel alignment (CKA)* [7] to measure the similarity of representations across clients. This metric is resistant to rotation and isotropic scaling in the representation space, allowing us to effectively measure the similarity of representations across clients.

With a little abuse of notations, we define $Z_i \in \mathbb{R}^{n_i \times k}$ and $Z_j \in \mathbb{R}^{n_j \times k}$ as two stacked representations (can be pre-projection representations or post-projector representations) on client i and j respectively. Here, n_i and n_j represent the number of samples on client i and client j respectively, and k the dimension of representations. The original linear CKA is used to calculate the similarity between representations generated by the same dataset but at the different stages in the model. However, in this paper, we use it to

measure the similarity of the representation of different clients in the same dimension, which is calculated as follows:

$$CKA_{linear}(Z_i, Z_j) = \frac{\text{vec}(\text{cov}(Z_i^T)) \cdot \text{vec}(\text{cov}(Z_j^T))}{\|\text{cov}(Z_i^T)\|_F \|\text{cov}(Z_j^T)\|_F}, \quad (1)$$

where $\text{cov}(\cdot)$ denotes the covariance matrices, $\|\cdot\|_F$ denotes the Frobenius norm. Higher linear CKA values indicate greater similarity between two representations of different clients in the same dimension.

Additionally, we adopt the within-class variance in [6], to measure the class-wise *separation* of representation on local clients. This metric is determined by the ratio of the average within-class cosine distance, denoted by \bar{d}_{within} , to the overall average cosine distance, denoted by \bar{d}_{total} . The one minus operation is performed to this ratio to get a closed-form index of class separation that is between 0 and 1, as follows:

$$R^2 = 1 - \frac{\bar{d}_{within}}{\bar{d}_{total}}. \quad (2)$$

Given an arbitrary client m , \bar{d}_{within} and \bar{d}_{total} are calculated as follows:

$$\bar{d}_{within} = \sum_{c=1}^C \sum_{i=1}^{N_m^c} \sum_{j=1}^{N_m^c} \frac{1 - z_m^{c,i} \odot z_m^{c,j}}{C(N_m^c)^2}, \quad (3)$$

$$\bar{d}_{total} = \sum_{c=1}^C \sum_{k=1}^C \sum_{i=1}^{N_m^c} \sum_{j=1}^{N_m^k} \frac{1 - z_m^{c,i} \odot z_m^{k,j}}{C^2 N_m^c N_m^k}, \quad (4)$$

where \odot is the cosine similarity, and N_m^c indicates the number of samples belonging to class C on client m .

Figure 2 presents the varying of R^2 during training. It can be seen that the personalized representations can achieve higher separation compared with the generalized representations. However, as shown in Figure 3, the similarity between clients of generalized representations is significant higher than that of the personalized representations. This demonstrates the DualFed can effectively decouple the optimization objectives of PFL (personalized federated learning) into two stages of the model representation extraction.

4.3 Comparison of Training Strategy

DualFed employs a stage-wise training strategy, ensuring that the pre-projection representation remain undisturbed by specific local

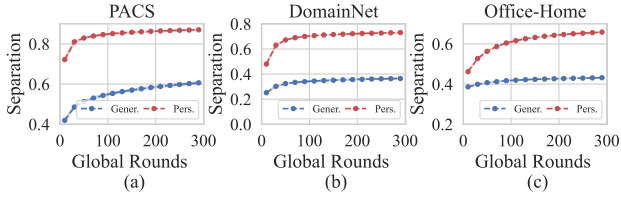


Figure 2: Class-wise separation during training.

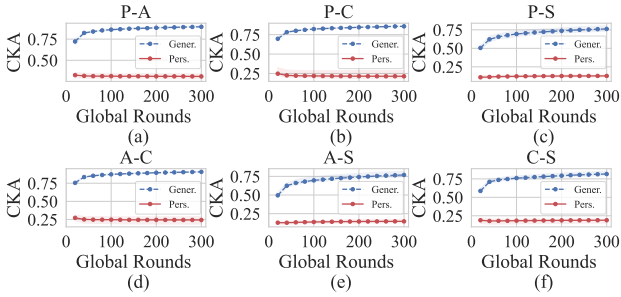


Figure 3: Client-wise CKA similarity during training.

tasks, thereby maintaining its generalization. Here, we compare this training strategy with the one that training all parameters simultaneously. Figure 4 presents the comparison of these two training strategies. As shown in Table 2, when E is relatively small (i.e., $E = 1$), simultaneous training can, in fact, outperform stage-wise training. However, as E increases (i.e., $E = 20$), simultaneous training lead to a obvious performance drop in PACS and DomainNet. This trend can be attributed to the fact that an increased number of local epochs causes the pre-projection representations to align more closely with the local task, thereby reducing their generalization.

Table 2: Experiments with Different Training Strategy.

E	Strategy	PACS	DomainNet	Office-Home
1	Stage-wise	95.01±0.31	86.14±0.12	79.74±0.37
	Simu.	95.15±0.16	86.68±0.20	80.57±0.09
20	Stage-wise	94.17±0.28	84.49±0.18	75.93±0.77
	Simu.	93.85±0.30	84.71±0.33	75.42±0.65

4.4 Effect of Position of Global Classifier

In DualFed, we employ a global classifier for generalized representations and a personalized classifier for personalized representations. Here we conduct experiments when placing the global classifier to the personalized representations. In these experiments, we maintain a shared encoder and investigated two configurations: sharing the projection network (DualFed-G) and personalizing it (DualFed-P). Figure 5 presents the differences of the above two configurations, along with the original DualFed. As indicated in Table 3, removing the global classifier to the same stage as the personalized classifier results in a significant performance decrease. This observation underscores the importance of the representations at different stages, as they provide complementary information (both generalized and

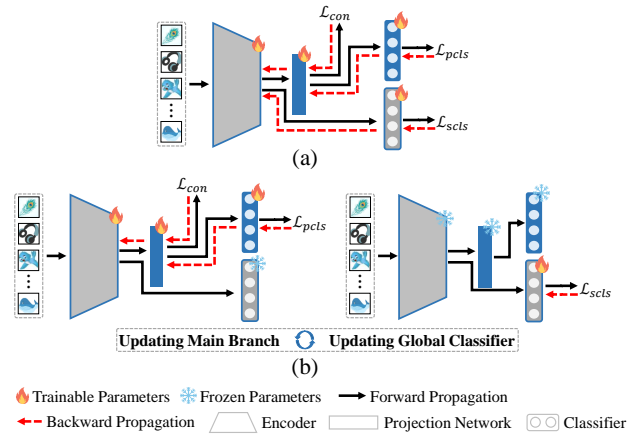


Figure 4: Illustration of different training strategies, (a) Simultaneous training, (b) Stage-wise training.

personalized information) that can enhance the overall performance of the model.

Table 3: Experimental Results when Placing Global Classifier at Different Positions.

	PACS	DomainNet	Office-Home
DualFed	95.01±0.31	86.14±0.12	79.74±0.37
DualFed-P	94.95±0.18	85.55±0.09	78.24±0.29
DualFed-G	94.84±0.12	84.90±0.42	78.08±0.17

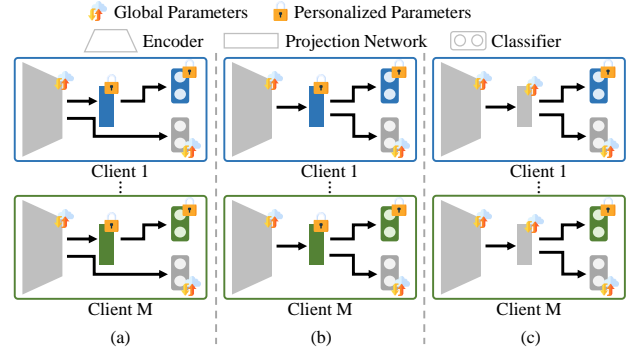


Figure 5: Illustration of different positions of the global classifier, (a) DualFed, (b) DualFed-P, (c) DualFed-G.

References

- [1] Manoj Guhan Arivazhagan, Vinay Aggarwal, Aaditya Kumar Singh, and Sunav Choudhary. 2019. Federated learning with personalization layers. *arXiv preprint arXiv:1912.00818* (2019).
- [2] Hong-You Chen and Wei-Lun Chao. 2022. On Bridging Generic and Personalized Federated Learning for Image Classification. In *International Conference on Learning Representations*.
- [3] Liam Collins, Hamed Hassani, Aryan Mokhtari, and Sanjay Shakkottai. 2021. Exploiting shared representations for personalized federated learning. In *International Conference on Machine Learning*. PMLR, 2089–2099.

- [4] Xin Dong, Sai Qian Zhang, Ang Li, and HT Kung. 2022. Sphered: Hyperspherical federated learning. In *European Conference on Computer Vision*. Springer, 165–184.
- [5] Kaiming He, Xiangyu Zhang, Shaoqing Ren, and Jian Sun. 2016. Deep residual learning for image recognition. In *Proceedings of the IEEE conference on computer vision and pattern recognition*. 770–778.
- [6] Simon Kornblith, Ting Chen, Honglak Lee, and Mohammad Norouzi. 2021. Why do better loss functions lead to less transferable features? *Advances in Neural Information Processing Systems* 34 (2021), 28648–28662.
- [7] Simon Kornblith, Mohammad Norouzi, Honglak Lee, and Geoffrey Hinton. 2019. Similarity of neural network representations revisited. In *International conference on machine learning*. PMLR, 3519–3529.
- [8] Da Li, Yongxin Yang, Yi-Zhe Song, and Timothy M Hospedales. 2017. Deeper, broader and artier domain generalization. In *Proceedings of the IEEE international conference on computer vision*. 5542–5550.
- [9] Tian Li, Anit Kumar Sahu, Manzil Zaheer, Maziar Sanjabi, Ameet Talwalkar, and Virginia Smith. 2020. Federated optimization in heterogeneous networks. *Proceedings of Machine learning and systems* 2 (2020), 429–450.
- [10] Xiaoxiao Li, Meirui JIANG, Xiaofei Zhang, Michael Kamp, and Qi Dou. 2021. FedBN: Federated Learning on Non-IID Features via Local Batch Normalization. In *International Conference on Learning Representations*.
- [11] Zexi Li, Xinyi Shang, Rui He, Tao Lin, and Chao Wu. 2023. No Fear of Classifier Biases: Neural Collapse Inspired Federated Learning with Synthetic and Fixed Classifier. In *Proceedings of the IEEE/CVF International Conference on Computer Vision (ICCV)*. 5319–5329.
- [12] Paul Pu Liang, Terrance Liu, Liu Ziyin, Nicholas B Allen, Randy P Auerbach, David Brent, Ruslan Salakhutdinov, and Louis-Philippe Morency. 2020. Think locally, act globally: Federated learning with local and global representations. *arXiv preprint arXiv:2001.01523* (2020).
- [13] Brendan McMahan, Eider Moore, Daniel Ramage, Seth Hampson, and Blaise Aguerre y Arcas. 2017. Communication-efficient learning of deep networks from decentralized data. In *Artificial intelligence and statistics*. PMLR, 1273–1282.
- [14] Adam Paszke, Sam Gross, Francisco Massa, Adam Lerer, James Bradbury, Gregory Chanan, Trevor Killeen, Zeming Lin, Natalia Gimelshein, Luca Antiga, et al. 2019. Pytorch: An imperative style, high-performance deep learning library. *Advances in neural information processing systems* 32 (2019).
- [15] Xingchao Peng, Qinxun Bai, Xide Xia, Zijun Huang, Kate Saenko, and Bo Wang. 2019. Moment matching for multi-source domain adaptation. In *Proceedings of the IEEE/CVF international conference on computer vision*. 1406–1415.
- [16] Yue Tan, Guodong Long, Lu Liu, Tianyi Zhou, Qinghua Lu, Jing Jiang, and Chengqi Zhang. 2022. Fedproto: Federated prototype learning across heterogeneous clients. In *Proceedings of the AAAI Conference on Artificial Intelligence*, Vol. 36. 8432–8440.
- [17] Hemanth Venkateswara, Jose Eusebio, Shayok Chakraborty, and Sethuraman Panchanathan. 2017. Deep hashing network for unsupervised domain adaptation. In *Proceedings of the IEEE conference on computer vision and pattern recognition*. 5018–5027.
- [18] Fu-En Yang, Chien-Yi Wang, and Yu-Chiang Frank Wang. 2023. Efficient model personalization in federated learning via client-specific prompt generation. In *Proceedings of the IEEE/CVF International Conference on Computer Vision*. 19159–19168.